EasyChair Preprint

№ 7103

Boundary Measurement for Axisymmetric Blunt Base Body by Numerical and Experimental Methods

The Hung Tran, Dinh Anh Le, Trang Minh Nguyen and Cong Truong Dao

November 28, 2021

Boundary measurement for axisymmetric blunt base body by numerical and experimental methods

The Hung Tran[1*], Dinh Anh Le[2], Trang Minh Nguyen[3], Cong Truong Dao[3]

[1]Faculty of Aerospace Engineering, Le Quy Don Technical University,
236 Hoang Quoc Viet, Bac Tu Liem, Hanoi, Vietnam

[2]School of Aerospace Engineering, University of Engineering and Technology, Vietnam National University (Hanoi)
334 Nguyen Trai, Thanh Xuan, Hanoi, Vietnam

[3]Academy of Military Science Technology, Lai Xa, Lai Xa, Bac Tu Liem, Hanoi, Vietnam

[*]Email: tranthehung_k24@lqdtu.edu.vn

Abstract. Boundary layer is known as a small layer around the moving object where velocity changes from zero to free-stream velocity. The layer is significant thin, which made difficult for measurement. In this study, we presented an advantage technique for measurement boundary layer of axisymmetric moving vehicles. The experiments were conducted by particle image velocimetry method to obtain the initial image data. Then, single-pixel resolution ensemble algorithm was applied to obtain boundary profile near the surface. We also conducted numerical simulation examine the ability of different turbulent model in extract velocity and boundary layer around the surface. The results indicated that the experimental method allows detailed boundary layer on the surface. Additionally, simulation shows close results to the experiments. The experimental technique is, then, can be applied for measure velocity close to the surface of moving objects such as unmanned aerial vehicle, car model. The results will help us understand flow around models in order to increase their performance as well as saving energy

Keywords: Boundary layer, PIV, numerical simulation, RANS.

1 Introduction

Moving vehicles are well-known topic for fluid mechanic researcher in many year. The complicated feature of the moving vehicles occurs from turbulent boundary layer, which occurs in almost cases in the life. Near the vehicles, a boundary layer is formed. The boundary layer is known as a small layer beginning from the model's surface, where the velocity of air is equals zeros, to a normal position, where air velocity reaches to free-stream conditions. Turbulent flow makes process of measuring boundary layer and simulating it becomes complicated because this layer is sufficiently thin with high velocity gradient in the flow conditions.

Previously, boundary layer measurement was mainly conducted by using hot-wire device [1]. However, putting some device on measurement region can disturb the flow fields and reduce accuracy of measurement. To overcome this problem, particle image velocimetry (PIV) provides a powerful technique in analyzing velocity fields. The working principle of PIV is to measure the displacement of small tracer particles over a short time interval. To obtain high resolution of flow behavior near the surface of model, single-pixel ensemble correlation algorithm can be applied for data processing [2].

The complicated feature of boundary layer is also made many difficult for numerical methods. In fact, Reynolds-averaged Navier-Stokes equations have been widely applied for studying fluids flow [3], [4]. However, turbulent models were used to simulate boundary layer profile. Additionally, the quality of mesh near the model's surface is very low to reduce its volume and reduce numerical time. Consequently, the accuracy of the numerical process is difficult to evaluated. In among of turbulent model, the k-ω SST model shows the most effective in predict the boundary layer profile. Although some limitation is existed, it is interesting to know how far the turbulent model can predict the velocity profile near the boundary layer.

In this study, the k-ω SST turbulent model was applied to analyze the boundary layer profile around an axisymmetric model at low-speed conditions. Results by the numerical method are compared with experimental data from PIV measurement. To obtain high accuracy of velocity profile around the surface of model and reduce uncertainty of measurement, the single-pixel ensemble correlation algorithm was developed for data processing. Results show that the experimental method allows detailed boundary layer on the surface. Numerical results show high agreement with experimental data under low-speed conditions. The experimental technique is, then, can be applied for measure velocity close to the surface of moving objects such as unmanned aerial vehicle, car model. Details of numerical process and data processing algorithm will be presented in this study.

2 Methodology

2.1 Numerical methods

This study applied finite volume methods for calculating flow fields around the model. The methods are applied to Navier-Stokes equations, which contains the continuous equation, three momentum equations and the energy equation. Since, the study is conducted for both subsonic and supersonic flow, we neglected energy equations in subsonic conditions. Additionally, averaged filters are applied to Navier-Stokes equations and only the steady flow are obtained. To overcome closure problem, additional equations are used. We use k-ω RANS turbulence model to simulate flow fields.

For studying boundary profile, we applied finite volume methods, which were written by Ansys Fluent software. The software was copyrighted by Faculty of Aerospace Engineering, Le Quy Don Technical University, Hanoi, Vietnam. Second order accuracy of special discretization was selected. The SIMPLE algorithm was applied for simulation. The air is considered as ideal gas and viscosity was Sutherland model.

2.2 Experimental methods and data processing

To measure the boundary layer, we applied PIV measurement technique. PIV is non-intrusive measurement technique, which allows to reconstruct the velocity distribution around the model. The setup for PIV measurement is shown in Fig. 1. In details, a smoke generator (LSG-500S) is fixed before the wind tunnel go generate smoke particles in the wind tunnel test. The smoke generator has five lazkin nozzles and can provide air with smoke particles of around 1 μm in diameter and 25 m^3/h in volume. We tried different test to choose the best time of experiment. In fact, the number of particles is sufficient for experimental study. The smoke particles are illuminated by a laser which was placed on the top of the test section. Movement of particles are captured by high speed camera for data processing. To synchronize the laser and high speed camera, a timing HUB and computer system is used. Since smoke particles are captured at different time, the movement of particles can be analyzed and velocity fields around the model can be obtained.

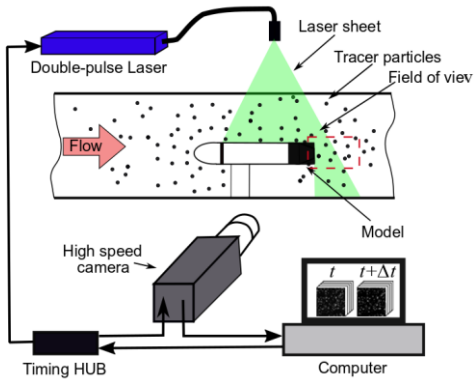

Fig. 1. Experimental setup for PIV measurement

For data processing, conventional PIV technique uses cross-correlation algorithm which processes in small interrogation window of the image frame. The size of interrogation window often ranges from 8×8 to 64×64 for good results. The resolution of the velocity fields is, therefore, reduce 64 to 4096 times by comparison to original image frame. Clearly, the results are not enough for boundary layer profile.

To overcome the disadvantage of conventional PIV algorithm, the single-pixel resolution ensemble correlation is used for data processing. The algorithm calculates cross-correlation coefficient for a single position of the first image and the interrogation windows in the second image from a group of double frames [5]. In more detailed, information of each pixel in the first serial images and second serial images from a huge number of images was collected. Then, cross-correlation of each pixel in the first images with the second images was calculated. As the results, the displacement of each pixel in the first serial images can be founds and velocity fields can be obtained. Clearly, by comparison to conventional PIV algorithm which uses spatial domain, the single-pixel resolution ensemble correlation uses temporal domain for calculating displacement of the particles. Since single pixel is processed separately, the resolution of velocity fields is the same with the size of image. Additionally, flow near the wall is measured highly accurate. The principles of the single-pixel ensemble correlation are shown in Fig. 2.

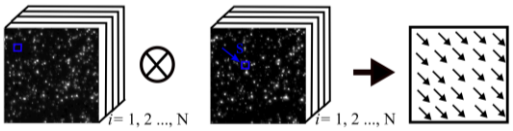

Fig. 2. Single-pixel ensemble correlation algorithm for data processing

The formula of cross-correlation in single-pixel ensemble correlation is shown as:

$$R(s) = \frac{1}{N}\sum_{i=1}^{N} I_1^{(i)}(X) I_2^{(i)}(X+s) \tag{1}$$

In this study, 2700 double-frame images are processed to obtain the average velocity field. Since the maximum displacement of particles from first to second frames is around 6 pixels, the displacement of each pixel in the first images was searched in a surrounding window of 20 × 20 pixels in the second image frames to reduce calculated time. The requirement of Random Access Memory (RAM) for calculation process is around 20 Gb. Numerical time around 1 day for each case. Typical image on experimental study is shown in Fig. 3.

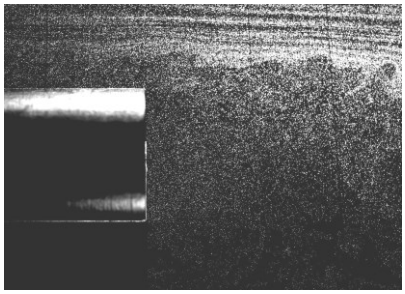

Fig. 3. Typical image taken during wind tunnel test

2.3 Model and flow conditions

To investigate boundary layer, we use an axisymemtric model, which has the same dimension to previous ones by Tran et al. [3]. The model has a diameter of 30 mm and a total length of 251 mm. The nose of model has ellipsoidal shape and the main part has cylinder shape. In experimental process, model is supported in wind tunnel by a strut support with cross-section of NACA 0018 (Fig. 1).

For numerical method, we selected a domain with a dimension of 5 D × 5 D × 33 D. The computation domain was divided into small blocks and meshed by hexahedron structure cells. The first layer on the model surface has height of 0.008 mm with the increasing ratio of 1.055. Mesh around the model is indicated in Figure 4. Total

number of cells of the domain is around 2.8 million. Effect of mesh size on numerical results was presented in previous study. For the detailed information, reader can refer to previous studies by Tran et al. [3], [6].

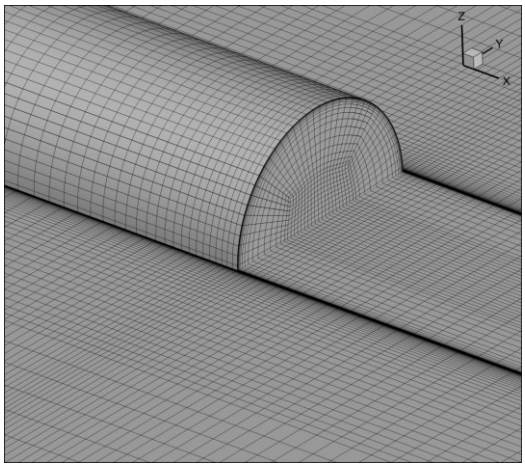

Fig. 4. Model configuration and mesh generation around the object

For both numerical and experimental studies, the free-stream velocity is fixed at 10 m/s. The velocity is sufficient small for good capture of smoke particles around the model. Additionally, the flow phenomenon was not highly different at low-speed flow. Consequently, the velocity of 10 m/s can be featured for other case at low-speed condition. We focus to flow around the base of the model, where turbulent boundary layer was observed. In the next section, results of boundary layer and flow around the base will be presented.

3 Results and discussions

3.1 Numerical results

We firstly show the flow around the base of the model by numerical simulation. Figure 5 illustrate flow around the model at velocity of 10 m/s in the symmetric plane. Clearly, small velocity observes around the nose of the model. At the base of the model, a reversed flow region is observed with a ring vortex. Although small velocity is observed near the surface of the model, it is difficult to observe the change of velocity gradient. Generally, the boundary layer profile is very thin. High resolution of mesh is required to capture detailed change of velocity there.

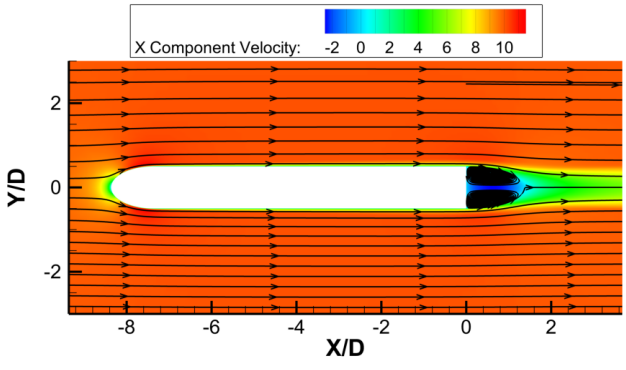

a.

Fig. 5. Velocity in symmetric plane around the model

Figure 6 shows distribution of pressure coefficient around the model. Clearly, by solving Navier-Stokes equations, all parameters of fluid flow can be obtained. It is a large advantage of numerical method by comparison to experimental one, where limited parameters are measured.

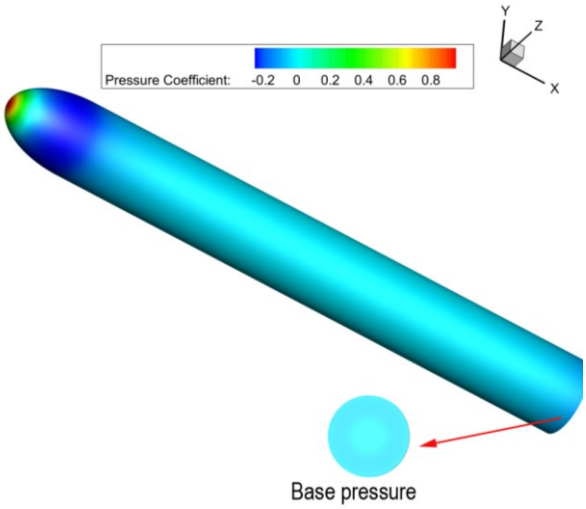

Fig. 6. Pressure distribution around the model

Figure 7 shows the boundary layer profile at different position on near the base surface. Since the model is symmetric, only velocity in *y* direction is illustrated. Here, the position *x/D* = 0 is the base edge. Interestingly, the boundary layer profile is similar for different position around the base. The thickness of boundary layer, where velocity reaches to 95% of free-stream velocity, is around 4 mm. The number of mesh layer near the surface of the model is sufficient to capture the velocity profile. It is expected that the flow behavior does not change much before the near-wake flow.

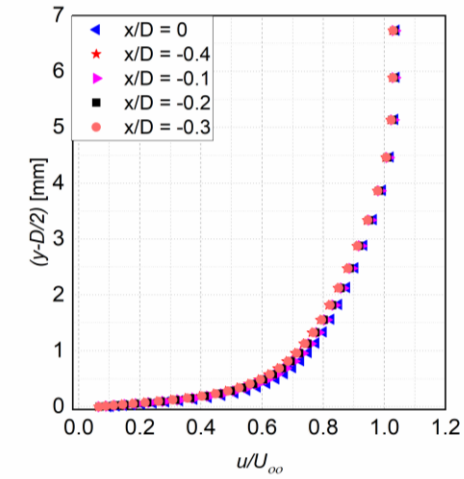

Fig. 7. Boundary layer profile at different position on the base by numerical methods

3.2 Experimental results

Now, the experimental results by the single-pixel ensemble correlation algorithm is presented. To obtain detailed velocity profile, different filters are applied to the results after the numerical process. Since, the results are processed on the images, only velocity profile on the symmetric plane is obtained. Figure 8 shows the velocity profile at the free-stream velocity of 10 m/s. The flow on the left bellow was not obtained because the smoke particles were not illustrated by the laser sheet. In the other words, the model hid by the laser sheet. Interestingly, clear velocity fields are obtained by the algorithm. The experimental results and numerical results

are highly consistent. It is expected that both methods can be applied to captured averaged flow fields around the model.

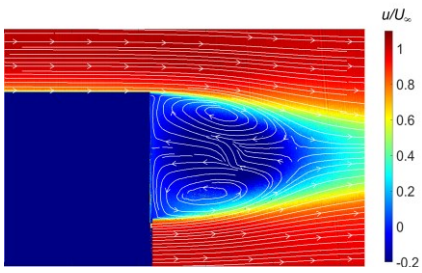

Fig. 8. Velocity fields around the base by the single-pixel ensemble correlation algorithm

Figure 9a shows the boundary layer profile by experimental methods for different positions around the base. Similar to numerical methods, boundary layer profiles show close profile for different positions. However, the number particle at (y - $D/2$) < 0.5 mm was quietly difficult to capture by experimental methods.

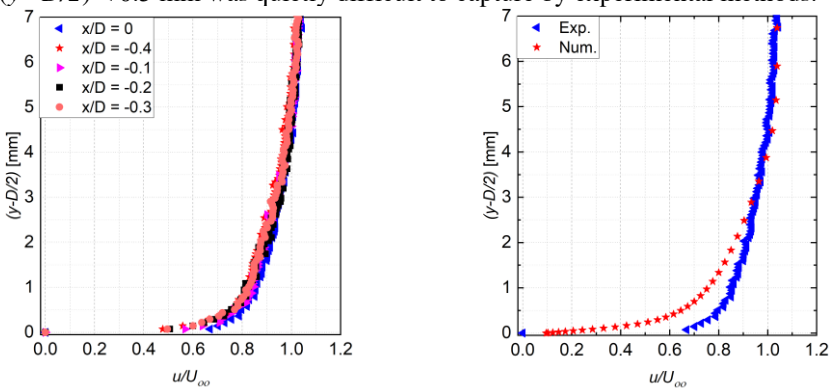

(a) Numerical method

(b) Compare between numerical and experiments at $x/D = 0$

Fig. 9. Boundary layer profile at different position on the base

3.3 Numerical and experimental comparison

To demonstrate the ability of both methods in analyzing boundary layer profile, we now compare experimental and numerical data. Figure 9b shows boundary layer profile at the position of $x/D = 0$ by both methods. Interestingly, the boundary layer far from the surface of the model is highly consistent for both methods. However, near the model's surface, small different results are obtained. It can be explained that the experimental results are affected by the number of smoke particles on the surface. On the other hand, numerical results are affected by turbulent models. Interestingly, the number of point by numerical methods are very high near the surface of the model. However, the number of point by the methods is very low far from the surface. The experimental results provide more measurement point by comparison to the numerical methods.

4 Conclusion

In this study, numerical and experimental methods were applied for analyzing boundary layer profile around an axisymmetric model under low-speed conditions. The numerical methods show high advantage in determining all parameters of the flow. On the other hand, data processing technique on images allow to capture velocity fields around the model. Although the experimental data allowed to capture only velocity profile, the resolution of the boundary layer near the model is very high. Both experimental and numerical methods showed a large wake structure behind the base surface. Additionally, the boundary layer profile did not change much before the base edge. Experimental and numerical results are highly consistent for velocity profile far from the model surface. However, near the surface of the model, both of them show some limitation. However, the k-ω turbulent

model and single-pixel ensemble correlation can be used for further study of boundary layer and the large wake structure.

References

[1] T. Lee, T. Nonomura, K. Asai, J. W. Naughton. Validation and uncertainty analysis of global luminescent oil-film skin-friction field measurement, Meas. Sci. Technol., 31(3) (2019) 35204.

[2] J. Westerweel, P. F. Geelhoed, R. Lindken. Single-pixel resolution ensemble correlation for micro-PIV applications, Exp. Fluids, 37(3) (2004) 375-384.

[3] T. H. Tran, H. Q. Dinh, H. Q. Chu, V. Q. Duong, C. Pham, and V. M. Do. Effect of boattail angle on near-wake flow and drag of axisymmetric models: a numerical approach, J. Mech. Sci. Technol., 35(2) (2021) 563-573. doi: 10.1007/s12206-021-0115-1.

[4] A. D. Le, H. Phan Thanh, H. Tran The. Assessment of a homogeneous model for simulating a cavitating flow in water under a wide range of temperatures, J. Fluids Eng., 143(10) (2021) 101204. doi: 10.1115/1.4051078.

[5] T. H. Tran, T. Ambo, T. Lee, L. Chen, T. Nonomura, K. Asai. Effect of boattail angles on the flow pattern on an axisymmetric afterbody surface at low speed, Exp. Therm. Fluid Sci., 99 (2018) 324-335. doi: 10.1016/j.expthermflusci.2018.07.034.

[6] T. H. Tran, L. Chen. Optical-flow algorithm for near-wake analysis of axisymmetric blunt-based body at low-speed conditions, J. Fluids Eng., 142(11) (2020) 1-10. doi: 10.1115/1.4048145.